Electronic Supplementary Material (ESI) for RSC Advances.

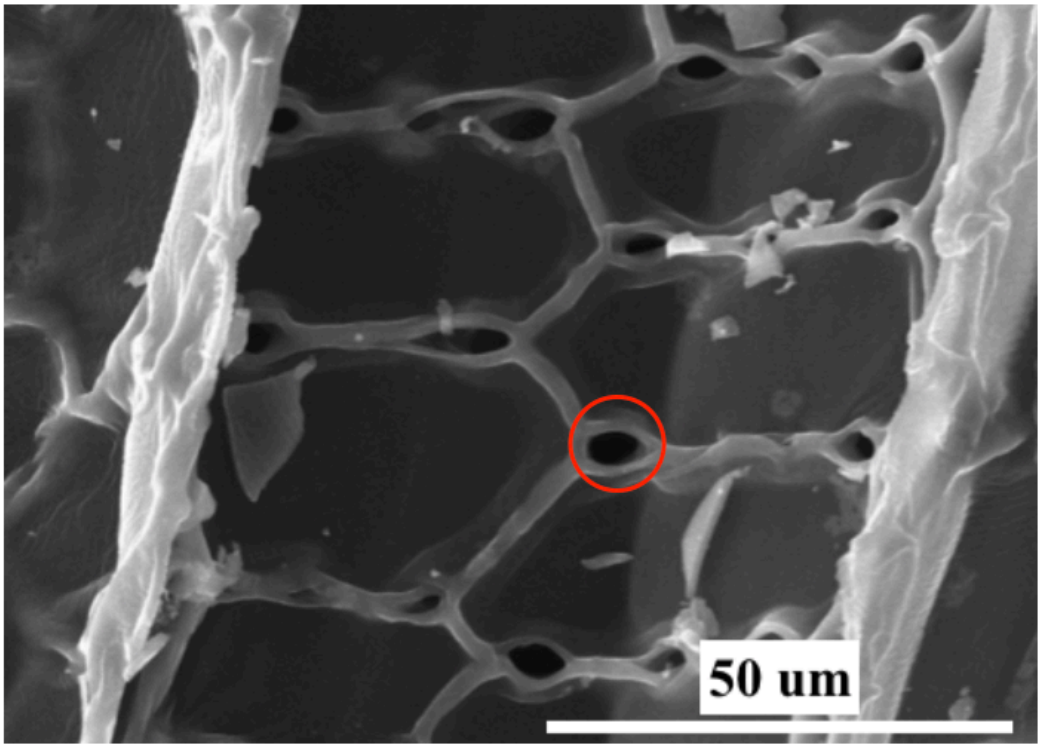

Supplementary Figure 1 - Higher magnification scanning electron microscopy (SEM) longitudinal image showing interconnecting pores in tubular structures (i.e. - red circle) of carbonized aerenchyma tissue which enables radial water transport in carbonized red mangrove root (RMR).

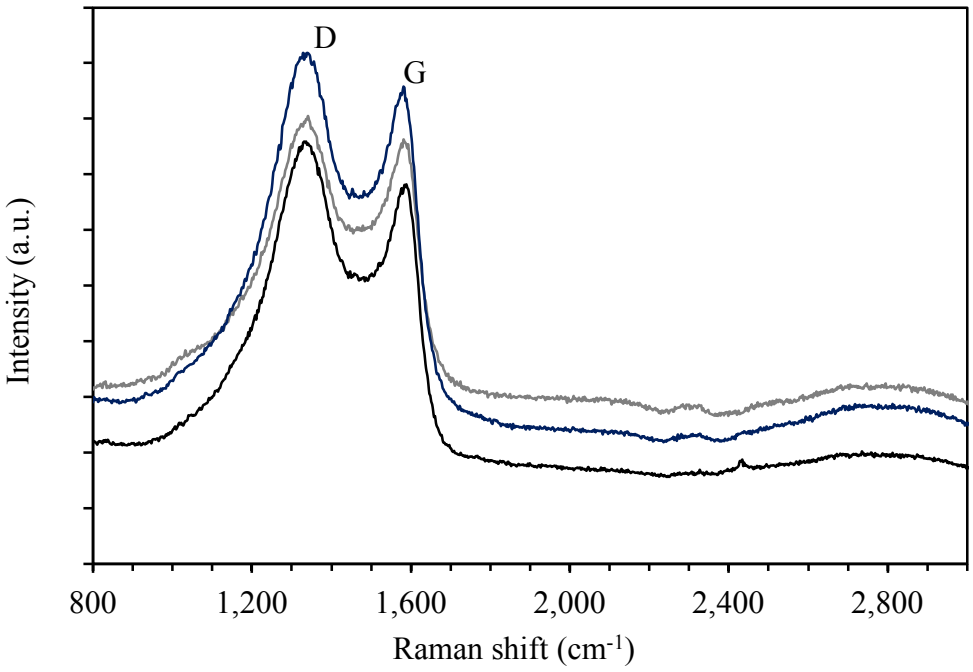

Supplementary Figure 2 – Raman spectra for three independently prepared carbonized RMRs. The units for the y-axis are arbitrary units (a.u.).

Supplementary Table 1 – Raman shift for D-band (disorder) and G-band (graphitic) at five separate locations on three independently prepared samples. Calculated I_d/I_g ratio was from peak intensity values.

	Sample 1			Sample 2			Sample 3		
Measurement	D-band	G-band	I_d/I_g	D-band	G-band	I_d/I_g	D-band	G-band	I_d/I_g
1	1336	1588	1.12	1336	1586	1.12	1346	1593	1.14
2	1333	1588	1.06	1341	1591	1.12	1336	1580	1.15
3	1331	1583	1.14	1336	1581	1.09	1336	1586	1.14
4	1331	1578	1.05	1338	1591	1.12	1333	1579	1.13
5	1338	1583	1.09	1336	1583	1.10	1336	1579	1.09

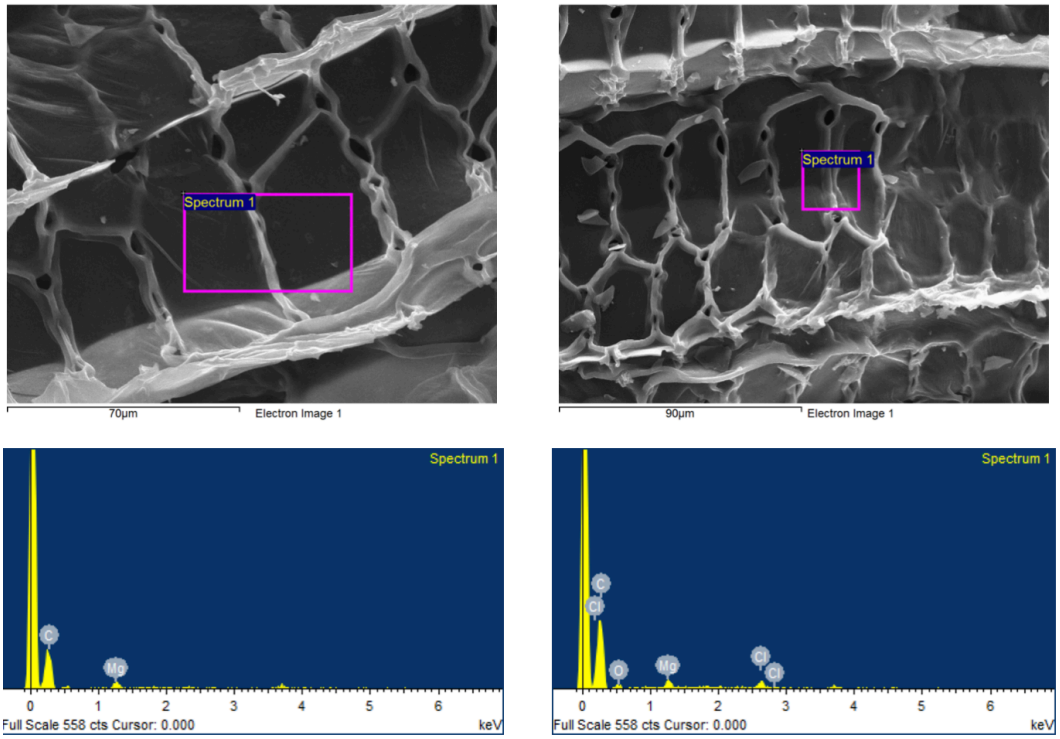

Supplementary Figure 3 – Representative sample of element identification by energy dispersive X-ray (EDX) spectroscopy in carbonized RMR aerenchyma. Outlined purple box indicates region of interest in elemental identification.

Supplementary Table 2 - EDX analysis at three locations on four independently prepared carbonized RMRs. Each sample exhibits high C content accompanied by the presence of Mg in at least two locations (ND = no detection).

	Sample 1			Sample 2			Sample 3			Sample 4		
Element (wt%)	#1	#2	#3	#1	#2	#3	#1	#2	#3	#1	#2	#3
C	93.90	95.26	95.26	75.49	83.64	78.90	93.47	93.07	95.50	93.47	93.07	95.50
Mg	6.10	4.74	4.74	2.88	2.70	2.89	2.34	1.09	ND	2.34	2.12	ND
O	ND	ND	ND	17.50	11.04	15.25	ND	ND	ND	ND	ND	ND
Cl	ND	ND	ND	2.47	2.62	2.97	4.19	4.81	4.50	4.19	4.81	4.50
Ca	ND	ND	ND	1.67	ND	ND	ND	ND	ND	ND	ND	ND

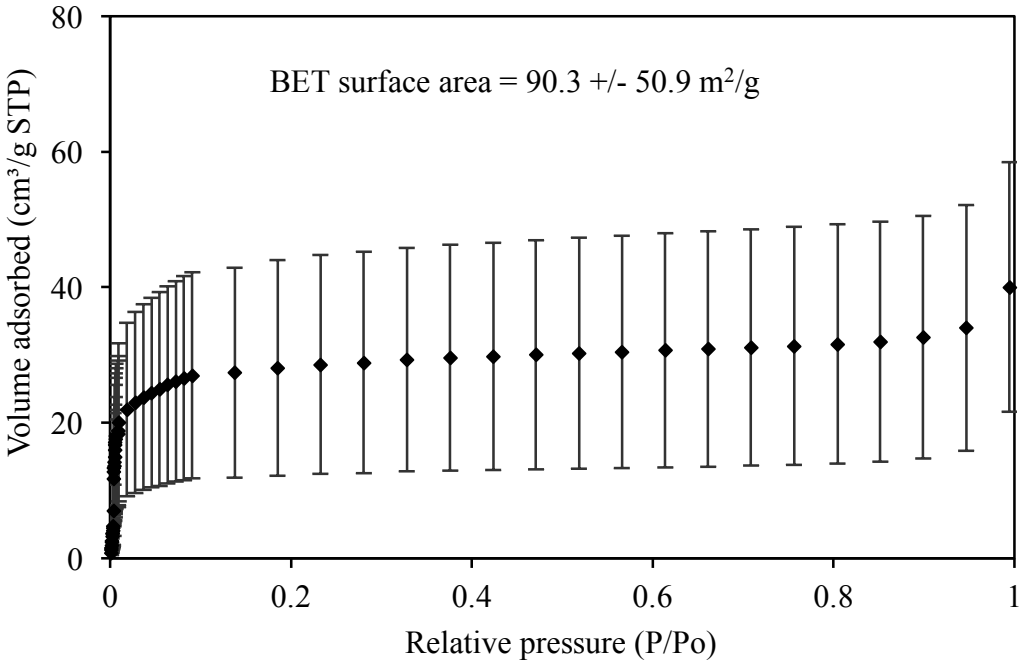

Supplementary Figure 4 – Nitrogen adsorption isotherm for carbonized RMRs. Mean +/- s.e.m., n=4 independent experiments.

a

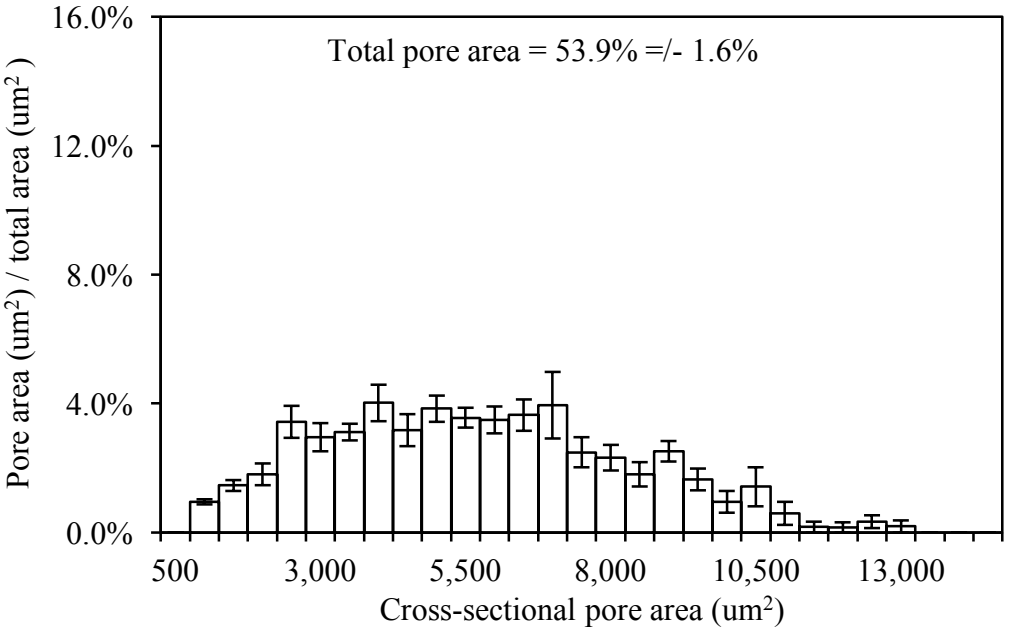

b

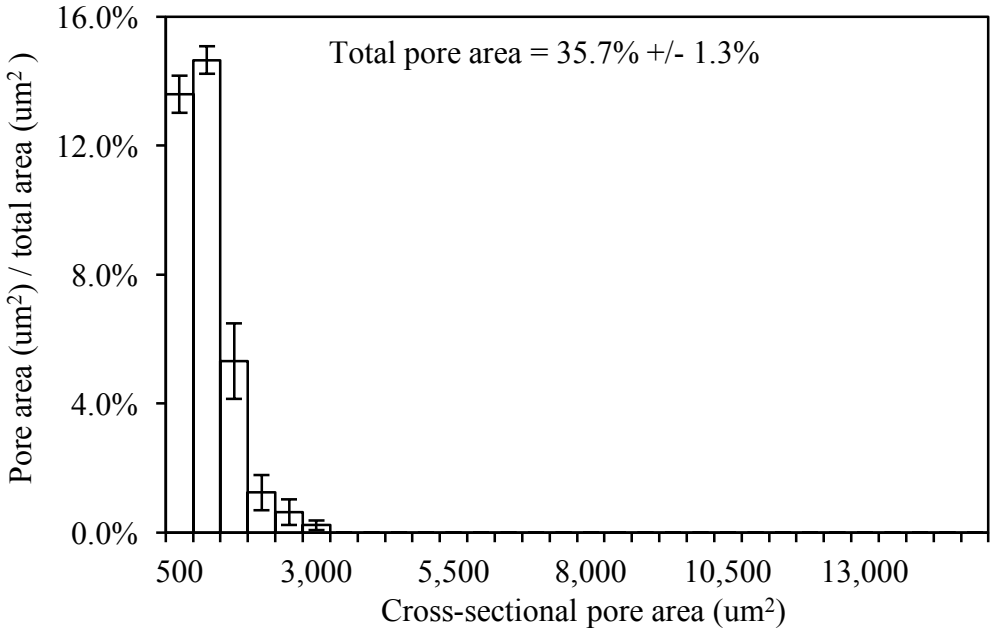

Supplementary Figure 5 - Cross-sectional area distribution of tube-like structures in (a) the aerenchyma of carbonized RMR and (b) the secondary xylem of carbonized common woody biomass. The average cross-sectional area of the tube-like structures in the carbonized RMR is approximately 10 times larger than that in the carbonized common woody biomass. Mean +/- s.e.m., n=5 (carbonized RMR) and n=3 (carbonized common woody biomass) independent experiments.

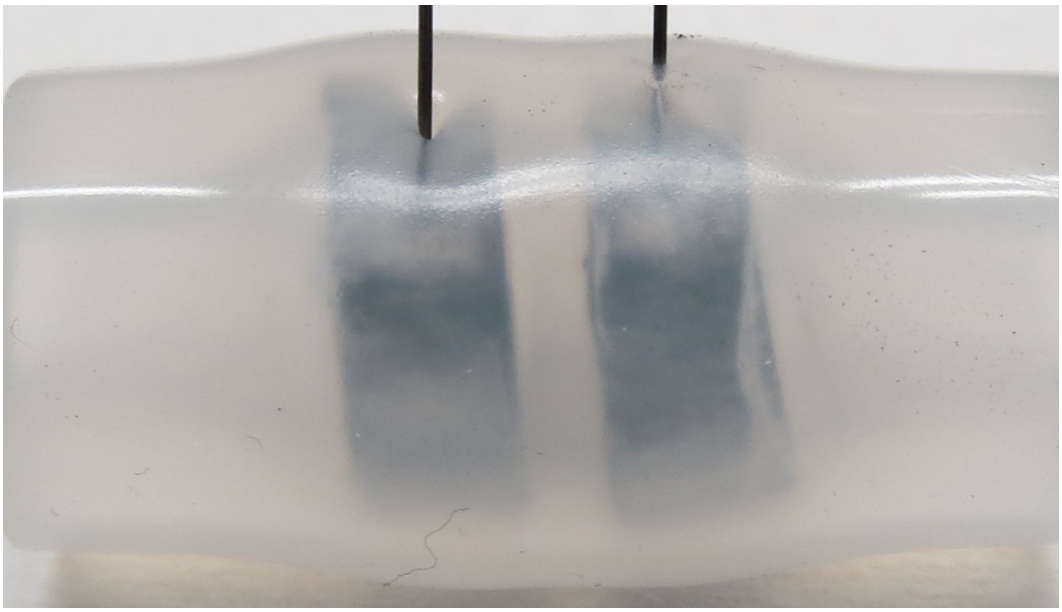

Supplementary Figure 6 – Mangrove-based FT-CDI cell. Two carbonized RMRs arranged in series in a custom-fabricated silicone coupling and connected to a power supply via 0.3 mm graphite rods.

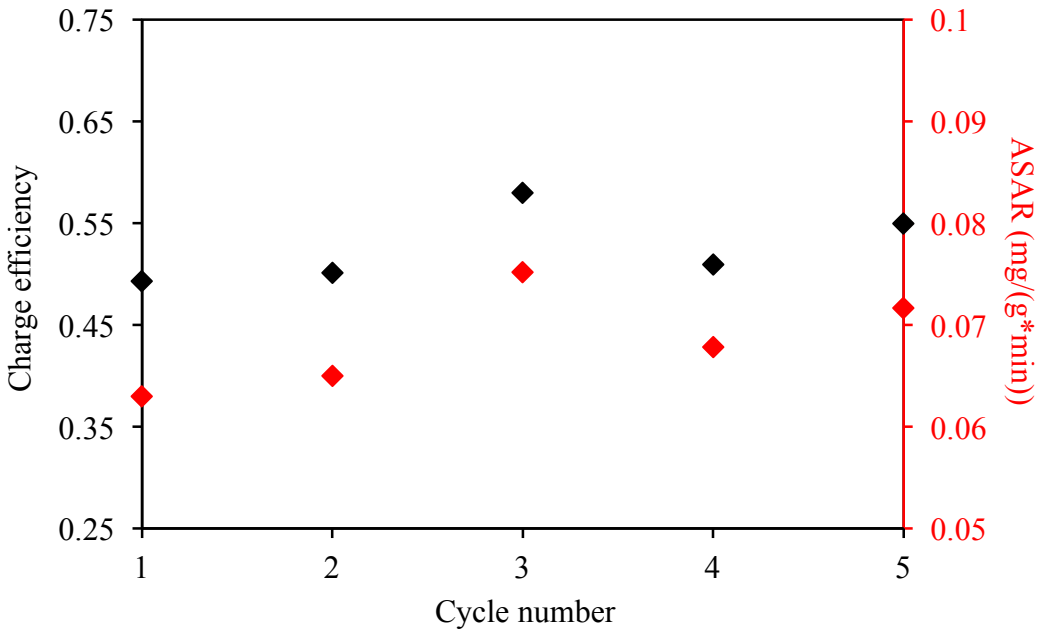

Supplementary Figure 7 – Charge efficiency and average salt adsorption rate (ASAR) for each cycle during cyclic operation. Charge efficiency (black diamonds) and ASAR (red diamonds) trended upward after first cycle.

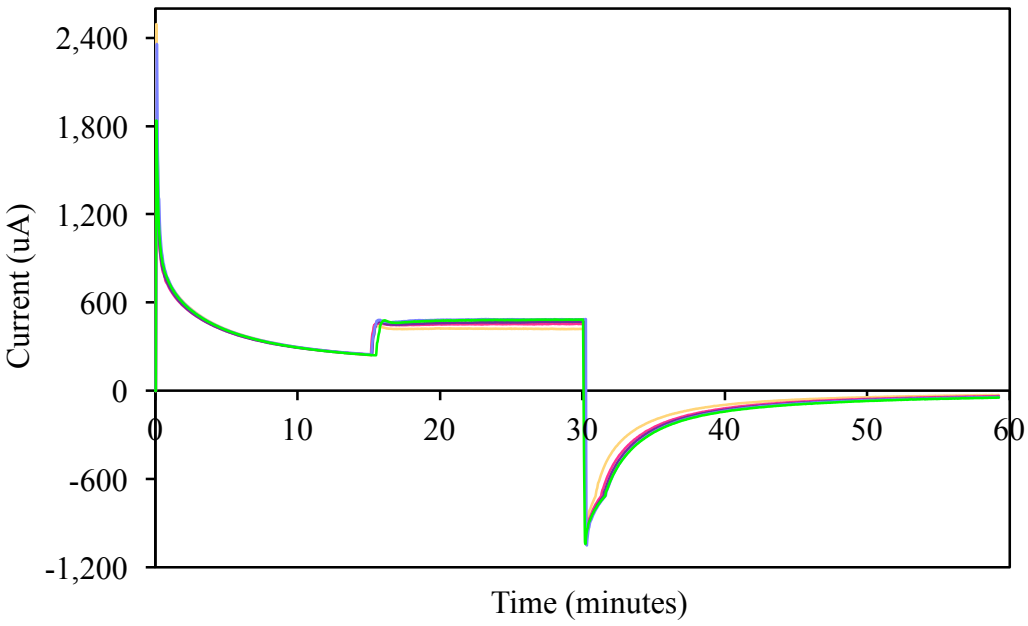

Supplementary Figure 8 - Charge/discharge current response from cyclic operation of bioinspired FT-CDI system. Initial capacitive current response for first 15 minutes corresponds to stopped-flow charging phase. Current response from 15 to 30 minutes corresponds to charging phase when flow is initiated (0.475 mL/min) while maintaining a potential of 1.5 V. Current response from 30 to 60 minutes corresponds to discharging phase at a flow rate of 0.475 mL/min and 0 V. (cycle 1 = orange; cycle 2 = pink; cycle 3 = purple, cycle 4 = light blue; cycle 5 = green)

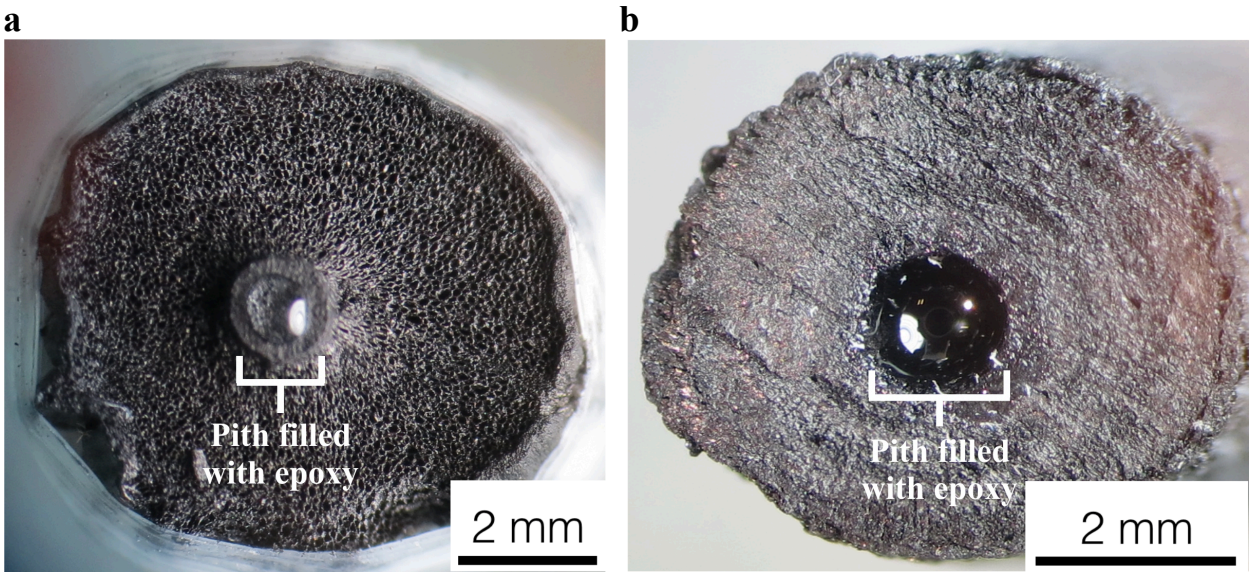

Supplementary Figure 9 – Representative cross-sectional image of (a) carbonized RMR and (b) carbonized common woody biomass with epoxy filled pith.

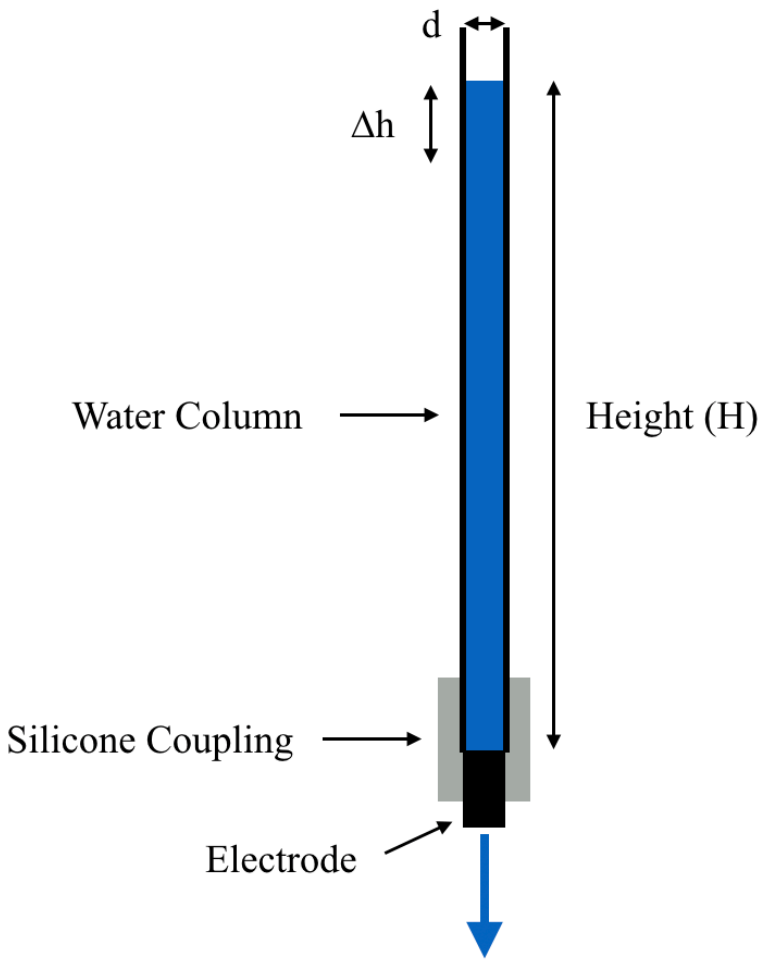

Supplementary Figure 10 – Schematic of experimental setup for constant pressure hydraulic permeability experiments.

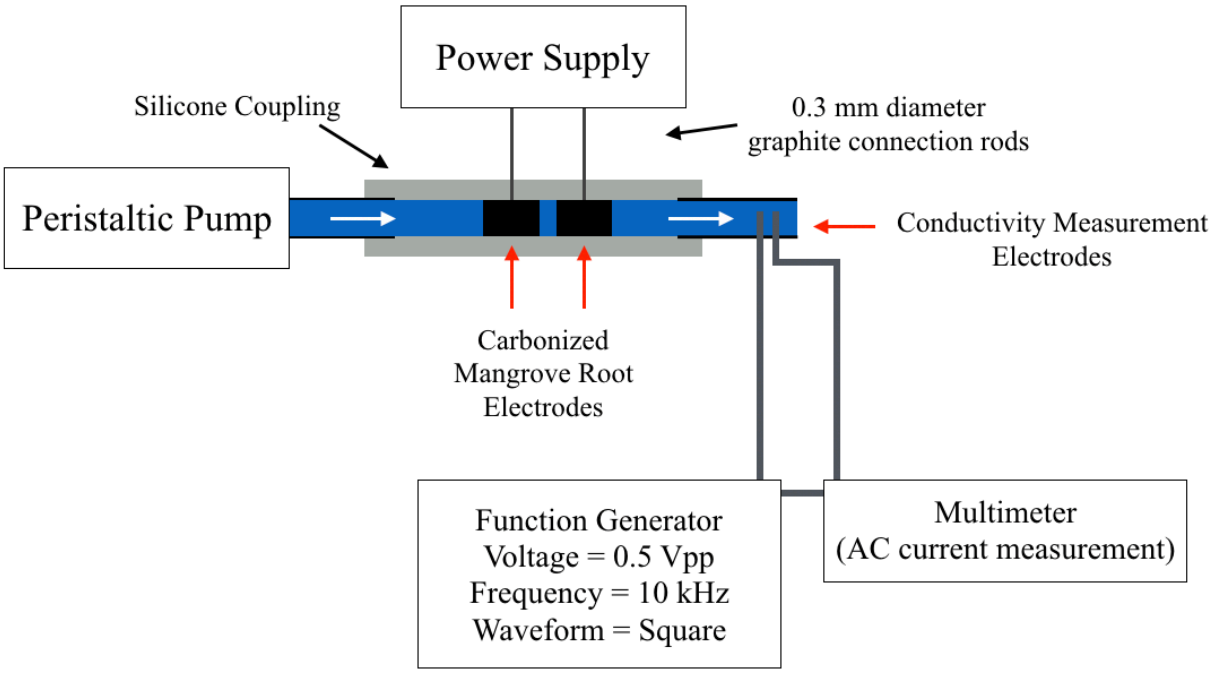

Supplementary Figure 11 – Schematic of FT-CDI experimental setup utilizing carbonized RMRs as highly permeable electrodes.

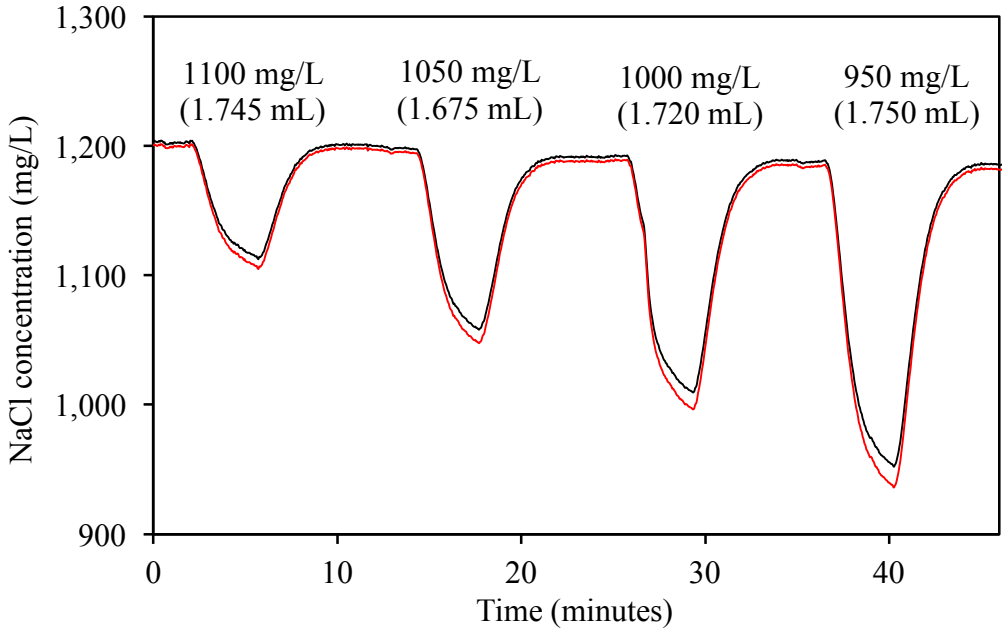

Supplementary Figure 12 - NaCl adsorption and concentration reduction control experiment examining the accuracy of the adsorption calculation method and conductivity meter. A 1200 mg/L NaCl solution was delivered through the flow-through capacitive deionization system in the absence of the carbonized red mangrove roots at a flow rate of 0.475 mL/min using a peristaltic pump. The inlet of the peristaltic pump was briefly inserted into a reservoir containing a NaCl solution of 1100, 1050, 1000, or 950 mg/L for approximately 3.7 minutes and then inserted back into the stock reservoir of 1200 mg/L. The reduction in NaCl concentration, which is similar to the concentration curves in Figure 4a, is indirectly measured using a flow-through conductivity meter and calculated from a calibration curve performed both before (Pre-run Calibration = black line) and after (Post-run Calibration = red line) the experiment shown above.

Supplementary Table 3 – NaCl adsorption control calculation from Supplementary Figure 12.

NaCl (mg)	1100 mg/L (1.745 mL)	1050 mg/L (1.675 mL)	1000 mg/L (1.720 mL)	950 mg/L (1.750 mL)
Actual	0.175	0.251	0.344	0.438
Pre-run Cal.	0.158	0.234	0.320	0.431
Post-run Cal.	0.168	0.246	0.340	0.451
Error (%)				
Pre-run Cal.	-9.3%	-6.9%	-6.9%	-1.6%
Post-run Cal.	-4.0%	-2.2%	-1.2%	3.0%

Supplementary Table 4 – NaCl concentration reduction control from Supplementary Figure 12.

NaCl (mg/L)	1100 mg/L (1.745 mL)	1050 mg/L (1.675 mL)	1000 mg/L (1.720 mL)	950 mg/L (1.750 mL)
Actual	100	150	200	250
Pre-run Cal.	90	139	181	235
Post-run Cal.	95	146	192	249
Error (%)				
Pre-run Cal.	-10.0%	-7.3%	-9.5%	-6.0%
Post-run Cal.	-5.0%	-2.7%	-4.0%	-0.4%